Neurobiology of Disease

β-Secretase-Cleaved Amyloid Precursor Protein Accumulates at Actin Inclusions Induced in Neurons by Stress or Amyloid β: A Feedforward Mechanism for Alzheimer's Disease

Michael T. Maloney, Laurie S. Minamide, Andrew W. Kinley, Judith A. Boyle, and James R. Bamburg

Department of Biochemistry and Molecular Biology, Program in Molecular, Cellular, and Integrative Neuroscience, Colorado State University, Fort Collins, Colorado 80523

Rod-like inclusions (rods), composed of actin saturated with actin depolymerizing factor (ADF)/cofilin, are induced in hippocampal neurons by ATP depletion, oxidative stress, and excess glutamate and occur in close proximity to senile plaques in human Alzheimer's disease (AD) brain (Minamide et al., 2000). Here, we show rods are found in brains from transgenic AD mice. Soluble forms of amyloid β ($A\beta_{1-42}$) induce the formation of rods in a maximum of 19% of cultured hippocampal neurons in a time- and concentration-dependent manner. Approximately one-half of the responding neurons develop rods within 6 h or with as little as 10 nM $A\beta_{1-42}$. $A\beta_{1-42}$ induces the activation (dephosphorylation) of ADF/cofilin in neurons that form rods. Vesicles containing amyloid precursor protein (APP), β-amyloid cleavage enzyme, and presenilin-1, a component of the γ-secretase complex, accumulate at rods. The β-secretase-cleaved APP (either β-C-terminal fragment of APP or Aβ) also accumulates at rods. These results suggest that rods, formed in response to either Aβ or some other stress, block the transport of APP and enzymes involved in its processing to Aβ. These stalled vesicles may provide a site for producing $A\beta_{1-42}$, which may in turn induce more rods in surrounding neurons, and expand the degenerative zone resulting in plaque formation.

Key words: **ADF/cofilin; actin; neurite inclusions; Alzheimer's disease; transport; APP processing; amyloid β**

Introduction

Hippocampal neurons exposed to neurodegenerative stimuli rapidly reorganize their actin cytoskeleton into rods, which are tapered cylindrical filamentous inclusions saturated with actin depolymerizing factor (ADF)/cofilin (Minamide et al., 2000). Rods form in neurons transiently exposed to treatments that mimic oxidative stress, excitotoxicity and ischemia, and their formation is accompanied by a net dephosphorylation (activation) of ADF and cofilin, two closely related protein regulators of actin dynamics in eukaryotic cells (Bamburg and Wiggan, 2002). Rods can occlude the neurite, disrupting microtubules and causing distal neurite atrophy (Minamide et al., 2000). Rod-like inclusions stained with ADF/cofilin antibody occur in human Alzheimer's disease (AD) brain. Almost all amyloid-rich senile plaques were associated with rod-like inclusions, but >40% of inclusions were not plaque associated. Thus, rods might occur in response to amyloid toxicity and/or they might participate in amyloid production.

Proteolytic cleavage of the full-length amyloid precursor protein (APP) by β-amyloid cleavage enzyme (BACE; also called β-secretase) and γ-secretase gives rise to amyloid β (Aβ) peptides (Price et al., 1995; Sisodia and Price, 1995; Hardy and Selkoe, 2002; Mattson, 2004; Tanzi and Bertram, 2005). Mutations leading to increased production of the more amyloidogenic $A\beta_{1-42}$ species are linked to early-onset familial AD (FAD) (Chartier-Harlin et al., 1991a,b; Goate et al., 1991; Murrell et al., 1991; Price et al., 1995). Treatment of cultured neurons with $A\beta_{1-42}$ inhibits fast axonal transport (Hiruma et al., 2003). Furthermore, blockage of axonal transport is the earliest measured disturbance in the brains of transgenic mice expressing mutant human APP (Stokin et al., 2005).

$A\beta_{1-42}$ can exist as monomers, oligomers, fibrils, and insoluble aggregates (Lambert et al., 1998; Walsh et al., 1999, 2002b; Dahlgren et al., 2002; Chromy et al., 2003; Kim et al., 2003). These various species possess different degrees of neurotoxicity. Fibrils increase reactive oxygen species (Harris et al., 1995; Cafe et al., 1996), lipid peroxidation, and free radicals (Hensley et al., 1996; Lim et al., 2005). Yet, soluble Aβ oligomers, including amyloid-derived diffusible ligands (ADDLs), are more neurotoxic than fibrils and insoluble larger aggregates (Dahlgren et al., 2002;

Received July 20, 2005; revised Oct. 18, 2005; accepted Oct. 20, 2005.

This work was supported by Alzheimer's Association Grant IIRG-01-2730, National Institutes of Health Grants NS40371, NS43115, and GM35126, and a grant-in-aid from Sigma Xi. We thank Drs. Yunfeng Lu and Bruce Parkinson for assistance with atomic force microscopy, Hilary Bowden for assistance with microscopy, and Dr. Barbara Bernstein, Dr. O'Neil Wiggan, Dr. Joe Fass, Kevin Flynn, and Alisa Shaw for valuable suggestions and assistance. We especially thank Chi Pak for suggestions and critical reading of this manuscript. We declare that they have no competing financial interests.

Correspondence should be addressed to Dr. James R. Bamburg, Department of Biochemistry and Molecular Biology, Colorado State University, Fort Collins, CO 80523-1870. E-mail: jbamburg@lamar.colostate.edu.

DOI:10.1523/JNEUROSCI.3711-05.2005

 0270-6474/05/2511313-09$15.00/0

Gong et al., 2003). Soluble Aβ and ADDLs at submicromolar concentrations are neurotoxic in organotypic cultures (Lambert et al., 1998), alter neuronal electrophysiology (Hartley et al., 1999), inhibit long-term potentiation (Walsh et al., 2002a), and cause transient memory deficits (Cleary et al., 2005). Together, these findings suggest that rod formation, initiated by Aβ peptides, might be the cause of transport blockage, which would affect synaptic function. Inhibition of transport also could enhance Aβ production, because the majority of β-secretase-cleaved APP occurs in endosomes (Koo and Squazzo, 1994; Yamazaki et al., 1995; Cordy et al., 2003; Ehehalt et al., 2003). Thus, rods may both initiate neurodegeneration and amplify accumulating degenerative signals (e.g., Aβ).

Here, we demonstrate that soluble $A\beta_{1-42}$ activates ADF/cofilin and induces the formation of rods in a subpopulation of cultured hippocampal neurons in a time- and concentration-dependent manner. Rods are sites where vesicles containing APP and β-secretase-cleaved APP accumulate.

Materials and Methods

All chemicals were reagent grade and obtained from Sigma-Aldrich (St. Louis, MO), and all tissue culture reagents were from Life Technologies (Invitrogen, San Diego, CA). β-Amyloid peptides ($A\beta_{1-42}$ and a scrambled peptide with the same amino acid composition) were purchased from AnaSpec (San Jose, CA). AMS-F-12 medium with L-glutamine and without phenol red was purchased from Caisson Laboratories (Rexburg, ID).

$A\beta_{1-42}$ preparations

Solubilization of the β-amyloid peptides and generation of the different $A\beta_{1-42}$ aggregates were performed as described previously (Dahlgren et al., 2002; Stine et al., 2003). Fibril preparations were centrifuged for 15 min at room temperature at 20,000 × *g*. The peptides in aliquots from supernatant and pellet fractions were extracted for dot blot analysis as described previously (Stine et al., 2003). Primary antibody (FCA18; Oncogene Research Products, San Diego, CA), recognizing the N-terminal amino acid of $A\beta_{1-42}$, was used at 1:500 in blocking solution for 1 h at room temperature. Horseradish peroxidase-conjugated secondary antibody was used at 1:30,000 in Tris-buffered saline (TBS) plus 0.05% Tween 20 at room temperature for 1 h. Blots were developed using SuperSignal West Pico or Extended Duration Chemiluminescent substrates (Pierce, Rockford, IL). Digitized images were captured using a Photometrics (Tucson, AZ) CH250 CCD camera, and spot intensity was quantified using MetaMorph software (version 6.1r5; Universal Imaging Corporation, West Chester, PA).

Cell culture and treatments

Hippocampal neuronal cultures were prepared as described previously (Bartlett and Banker, 1984; Mattson and Kater, 1988; Minamide et al., 2000), with the following changes. Dissociated cells were plated on poly-D-lysine-coated substrates in 8-well Lab Tek chamber slides (Nalg Nunc International, Rochester, NY) and cultured under 400 μl of Neurobasal medium supplemented with B27 and glutamine in a humidified 95% air/5%CO_2 incubator at 37°C. Dissociated cultures enriched in CA1 or CA3 neurons were prepared from 400 μm slices (Mcilwein tissue chopper) of embryonic day 18 (E18) rat hippocampi (Meberg and Miller, 2003). Before dissociation, slices were further dissected into CA1 and CA3 regions on a Nikon (Melville, NY) SMZ-U dissection microscope, as shown in supplemental Fig. S1 (available at www.jneurosci.org as supplemental material). Hippocampal neurons [6 d *in vitro* (div)] were treated with 10 nM, 100 nM, or 1 μM $A\beta_{1-42}$ in the form of low-molecular weight (LMW) species, large oligomers, and fibrils/insoluble aggregates for 0.5–72 h. Controls included untreated neurons or neurons treated with 0.5% DMSO (vehicle) or with 1 μM scrambled Aβ peptide that had been preincubated under conditions in which $A\beta_{1-42}$ forms fibrils.

For some studies, rods were induced by transient (20 min) ATP depletion, followed by washout of the ATP-depletion medium and 24 h recovery (Minamide et al., 2000). Rods were also induced in some experiments by infecting 4 div hippocampal neuronal cultures with adenovirus for expressing the green fluorescent protein chimera of wild-type *Xenopus* ADF/cofilin (XAC-GFP) (Meberg and Bamburg, 2000). Spontaneous rods start to form in neurites of infected cells by 60 h after infection (B. W. Bernstein, H. Chen, J. A. Boyle, and J. R. Bamburg, unpublished results). Cells were fixed at 72 h after infection.

Cells were fixed 30 min in cytoskeleton preservation buffer (10 mM MES, pH 6.1, 138 mM KCl, 3 mM $MgCl_2$, 2 mM EGTA, and 0.32 M sucrose) containing 4% paraformaldehyde, pH 7.0. Cells were methanol (−20°C) permeabilized for 3 min and blocked in 2% goat serum/1% BSA in TBS before immunostaining with various antibodies. Primary antibodies included the following: affinity-purified rabbit antiserum to chick ADF (2 ng/μl), which cross-reacts with mammalian ADF and cofilin (Minamide et al., 2000); affinity-purified rabbit anti-phosphorylated ADF/cofilin (pAC; 0.02 ng/μl), which recognizes only the ser-3 phosphorylated forms of ADF/cofilin (Meberg et al., 1998); protein A-purified monoclonal mouse anti-cofilin (Mab22; 10 ng/μl IgG) (Abe et al., 1989); monoclonal anti-human β-amyloid Asp-1 (FCA18; 1:150; Oncogene Research Products); rabbit anti-BACE (M-83; 1:150; Santa Cruz Biotechnology, Santa Cruz, CA); rabbit anti-presenilin 1 (PS1; residues 31–46; Ab-1; 1:150; Oncogene Research Products); and rabbit anti-β-APP (1:150; Zymed, San Francisco, CA). Secondary antibodies, all used at 1:450, included fluorescein goat anti-rabbit, goat anti-mouse, Texas Red goat anti-rabbit, and Texas Red goat anti-mouse (Invitrogen). DAPI (4′-6-diamidino-2-phenylindole) was used at 1:1000 (Invitrogen). After blocking and staining, the rubber dividing chambers were removed, and a 24 × 50 mm coverglass was mounted with Prolong Gold Antifade (Invitrogen).

The relative level of pAC to total cofilin was determined by ratiometric analysis of fluorescence overlays from neurons immunostained with both pAC rabbit and mouse Mab22 primary antibodies and Texas Red and fluorescein secondary antibodies. Average pixel intensities were measured after background subtraction using MetaMorph software. All values were normalized to the ratio (set to 1) of pAC to total cofilin in untreated neurons.

Brain sections from transgenic (Tg2576) mice

A 4-month-old transgenic mouse (Tg2576; Taconic, Germantown, NY) was perfusion fixed (Bruijn et al., 1997), and the brain was removed, postfixed, and paraffin embedded. Sections (5 μm) were deparaffinized and immunostained for ADF/cofilin as reported previously for human AD brain (Minamide et al., 2000).

Microscopy

Light microscopy. Phase-contrast and fluorescence micrographs were obtained using a 60× [1.4 numerical aperture (NA)] oil objective as described previously (Minamide et al., 2000). Fluorescence measurements were made from nonsaturating digital images all acquired under the same conditions with a CoolSnap ES CCD (Photometrics). Quantitative analyses of some of these images was performed by obtaining average fluorescence intensities from the different cell regions (line scans) after subtracting background. MetaMorph v6.1 software (Universal Imaging) was used for all digital image processing. Slides were coded and scored blind to obtain percentages of neurons containing rods. At least 200 neurons per well were observed with a 40× oil (1.3 NA) objective, and the percentages of neurons containing rods were recorded. To quantify the percentage of neurons that survived, the total number of neurons in 10 randomly selected fields (20× air objective) from $A\beta_{1-42}$-treated cultures was counted per well. This number was compared with the number of neurons surviving from untreated cultures plated from the same neuronal stock. Averages and SDs for identical treatments were obtained from multiple wells. Experiments were repeated three or more times to give SEMs. ANOVA was performed using SAS/LAB software (SAS Institute, Cary, NC).

Electron microscopy. A 3 μl aliquot of $A\beta_{1-42}$ samples from each incubation condition was applied to a formvar-coated slot copper grid, blotted dry, negatively stained with 1% aqueous uranyl-acetate, and examined on a JEOL-2000 TEM (JEOL, Peabody, MA) at 100 kV. Postmortem human AD hippocampus (brain bank tissue) was fixed after removal in 4% paraformaldehyde and 2% glutaraldehyde and postfixed in osmium, dehydrated, and embedded in LR White resin; uranyl acetate/lead citrate-stained sections (90 nm) were observed with a JEOL-2000 TEM.

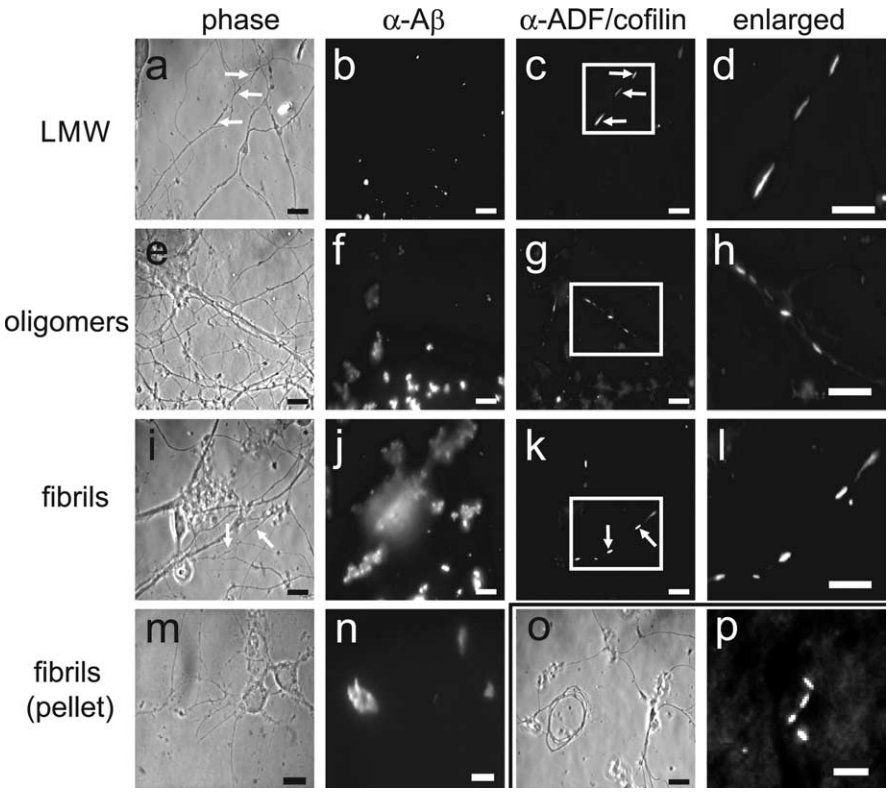

Figure 1. Aβ peptides induce rods in cultured neurons and in brains of transgenic mice. ***a–l***, Rods in hippocampal neurons treated with 1 μM $A\beta_{1-42}$ LMW, large oligomer (oligomers) or fibril/insoluble aggregate (fibrils) preparations. The arrows in ***a***, ***c***, ***i***, and ***k*** show the location of a rod in the phase and fluorescence image pairs. ***m***, ***n***, Neurons treated with the insoluble aggregates from the fibril preparations. Aβ immunofluorescence is more compact compared with whole fibril/insoluble aggregate preparations. ***o***, Example of a dystrophic neurite commonly found in fibril/insoluble aggregate-treated cultures. ***p***, Immunofluorescent rods stained for ADF/cofilin in the posterior cortex of a section of brain from a 4-month-old Tg2576 mouse. Scale bars: ***a–o***, 10 μm; ***p***, 5 μm.

Atomic force microscopy. Peptides were prepared for atomic force microscopy (AFM) as described previously (Stine et al., 2003). Images were obtained on NanoScope IIIa Scanning Probe microscope equipped with MultiMode head, E-series piezoceramic scanner, and AFM probe type of single-crystal silicon microcantilevers with 300 kHz resonant frequency and 40 N/m spring constant.

Results

Characterization of Aβ aggregates

To determine whether any forms of $A\beta_{1-42}$ could induce rods in cultured hippocampal neurons, we prepared and incubated stock solutions of synthetic $A\beta_{1-42}$ peptide under conditions shown previously to enrich preparations in LMW species, large oligomers, or fibrils with larger aggregates (Walsh et al., 2002b). The composition of each prepared sample was analyzed by electron microscopy and by AFM (supplemental Fig. S2, available at www.jneurosci.org as supplemental material). Our three peptide preparations contain species that appear similar in size and distribution to those described previously (Lambert et al., 1998; Walsh et al., 1999, 2002b; Dahlgren et al., 2002; Chromy et al., 2003; Stine et al., 2003). Overlap of $A\beta_{1-42}$ species occurs between preparations. Thus, we will define these samples as follows: (1) a LMW preparation containing small bead-like structures and aggregates; (2) a large oligomer preparation containing larger aggregates and short protofibrils; and (3) a fibril/insoluble aggregate preparation containing ribbon-like fibrils that remained in the supernatant after centrifugation at 20,000 × *g* for 15 min, as well as large amorphous aggregates that pelleted (supplemental Fig. S2, available at www.jneurosci.org as supplemental material). The insoluble aggregates of $A\beta_{1-42}$ look remarkably similar in size and shape to the aggregates that comprise the dense core senile plaques of human AD brain (supplemental Fig. S2, available at www.jneurosci.org as supplemental material).

Rods, which are straight tapered bundles of F-actin saturated with ADF/cofilin, were identified by immunostaining for ADF/cofilin in E18 rat hippocampal neurons (6 div) treated 24 h with 1 μM of each of the different $A\beta_{1-42}$ samples (Fig. 1). Although neurites containing rods are contiguous, methanol permeabilization left phase-dense regions where rods had formed (Fig. 1*a*, arrows), sometimes giving the neurites a fragmented appearance. In Triton X-100-extracted cultures (data not shown), the neurite morphology is maintained, and neurite fragmentation is not apparent (Minamide et al., 2000). Control neurons included those that were untreated, treated with vehicle alone (0.5% DMSO), or treated with 1 μM scrambled $A\beta_{1-42}$ peptide that had been preincubated identically to the fibril fraction of $A\beta_{1-42}$. Cultures were also stained with the human anti-Aβ (FCA18 directed against the N-terminal asp) antibody to monitor the distribution of $A\beta_{1-42}$ associated with the affected neurons. $A\beta_{1-42}$ immunostaining was dispersed randomly (Fig. 1*b*,*f*,*j*,*n*), but each of the different Aβ preparations resulted in distinctive immunofluorescence staining. LMW species appeared as discrete puncta, whereas large oligomers and fibrils/insoluble aggregates were more difficult to resolve in a single plane of focus. Tortuous and dystrophic neurites (Pike et al., 1992; Grace et al., 2002) were observed only in cultures treated with large oligomers and fibrils/insoluble aggregates (Fig. 1*o*).

The majority of extracellular Aβ is lost during fixation and immunostaining. However, large Aβ aggregates can be observed in cultures by phase microscopy (supplemental Fig. S3, available at www.jneurosci.org as supplemental material). Therefore, we analyzed the number of neurons in contact with visible Aβ aggregates by phase microscopy (20× objective) in live cultures. At any point in time, we determined that 31–41% of the neurons contacted phase-visible aggregates of Aβ when added at 1 μM. Furthermore, if we evaporated the medium from a treated culture before fixing and immunostaining for Aβ, between 52 and 65% of the neurites visualized by tubulin immunostaining were in direct contact with Aβ (supplemental Fig. S4, available at www.jneurosci.org as supplemental material). Because the large Aβ aggregates are freely moving in the culture medium, it is likely that all neurons spend at least some time in contact with Aβ aggregates *in vitro*.

Incubation conditions used to generate fibrils also generated insoluble aggregates (Lambert et al., 1998; Walsh et al., 1999, 2002b; Dahlgren et al., 2002; Chromy et al., 2003; Stine et al., 2003). To determine whether fibrils or insoluble aggregates were the rod-inducing species in this Aβ fraction, we separated the two

components by centrifugation at 20,000 × *g*. Portions of the supernatant and pellet fractions were solubilized in formic acid, and the amount of Aβ in each fraction was determined by an immuno-dot blot assay. Nearly all of the rod-inducing activity of the fibril/insoluble aggregate preparation was associated with the supernatant fraction containing fibrils (Fig. 2*a*) and not with the pellet fraction containing insoluble aggregates.

To determine whether excess Aβ production *in vivo* could also lead to neuronal rod formation, we examined the brain of a 4-month-old Tg2576 transgenic mouse for the presence of rods. Tg2576 mice express the Swedish mutation for human APP (Hsiao et al., 1996), which has been linked to FAD. A different strain of mouse expressing this same mutation of human APP generates excess Aβ peptides and has axonal transport deficits early in its development (Stokin et al., 2005). Brain sections from the perfusion-fixed Tg2576 mouse show the presence of ADF/cofilin immunostained rods (Fig. 1*p*). Other studies have confirmed the formation of ADF/cofilin-stained inclusions in neurons surrounding the regions of amyloid deposition in the Tg2576 mice (A. Mendoza-Naranjo, C. Otth, Bamburg, R. B. Maccioni, and C. Gonzalez-Billault, unpublished observations), similar to what has been observed in Alzheimer's brain (Minamide et al., 2000).

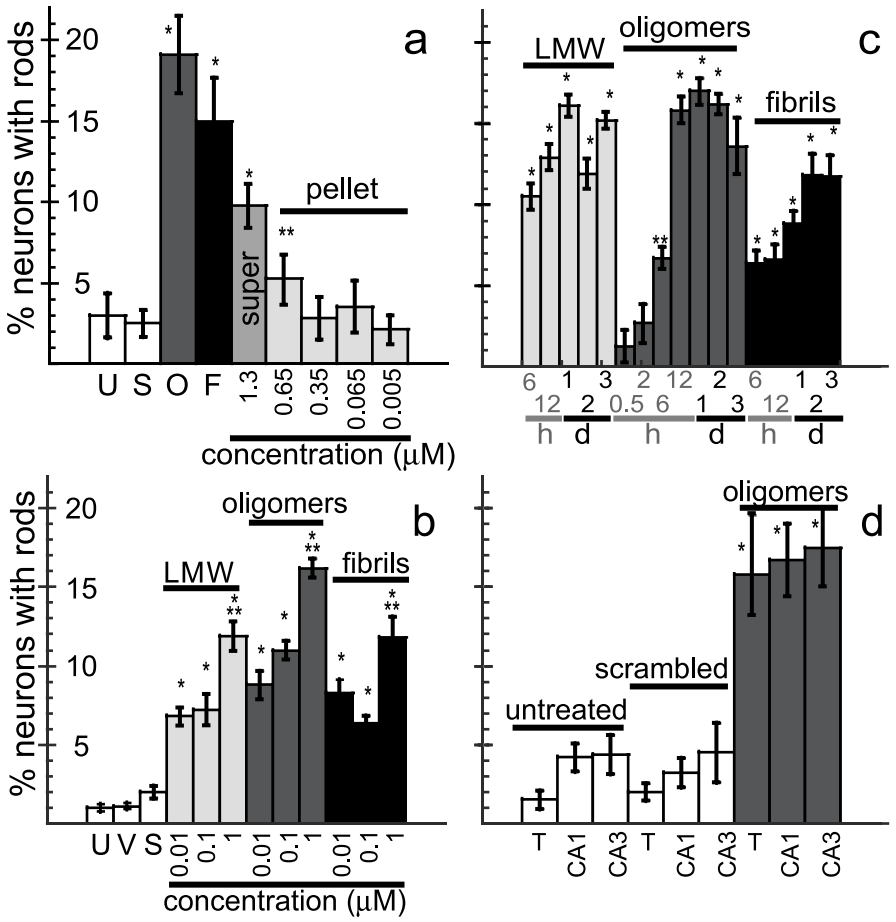

Figure 2. Effects of $A\beta_{1-42}$ on rod formation in cultured hippocampal neurons. ***a***, Percentage of neurons with rods after 48 h of exposure to Aβ peptides. $^{*}p < 0.0001$ and $^{**}p < 0.01$, significant differences between experimental and untreated controls. super, Supernatant. ***b***, Percentage of neurons with rods after 48 h of exposure to soluble Aβ forms. $^{*}p < 0.0001$, significant differences between experimental and untreated controls; $^{**}p < 0.005$, significant differences between experimental and other concentrations within its group. ***c***, Time course of 1 μM Aβ-induced rod formation. The time is in hours (h) and days (d). $^{*}p < 0.0001$ and $^{**}p < 0.001$, significant differences between experimental and untreated controls. ***d***, Neurons forming rods in response to 48 h Aβ treatment (1 μM oligomer) are equally within CA1 and CA3 regions of hippocampus. $^{*}p < 0.0001$, significant differences between experimental and untreated controls. Error bars indicate SEM. U, Untreated; S, scrambled peptide; O, large oligomers; F, fibrils/insoluble aggregates; V, vehicle (0.5% DMSO); T, total hippocampal neurons from a normal dissection.

$A\beta_{1-42}$ induces rods in a concentration- and time-dependent manner

To further characterize the rod-inducing activities of the $A\beta_{1-42}$ preparations, we examined their concentration dependence on rod formation in 6 div hippocampal neurons. Controls were identical to those described previously. Less than 2% of neurons contained rods in all control groups (Fig. 2*b*). LMW, large oligomer, and fibril/insoluble aggregate preparations of $A\beta_{1-42}$ between 10 nM and 1 μM induced a concentration-dependent increase in the percentage of neurons containing rods, with ~19% constituting the maximal response (Fig. 2*a*,*b*). All three Aβ preparations induced rods at 10 nM, the lowest concentration tested (Fig. 2*b*), although only approximately one-half of the maximal percentage response was observed. At or below 1 μM $A\beta_{1-42}$, neuronal survival at 48 h remained high (>80%). Rod formation and survival were also analyzed in neurons treated with 2 and 10 μM $A\beta_{1-42}$ large oligomers. The percentage of neurons forming rods did not increase at concentrations >1 μM; however, neuron survival declined considerably by 48 h after 2 μM treatment, and all neurons were dead after treatment with 10 μM $A\beta_{1-42}$. These findings suggest that a subpopulation of hippocampal neurons is very sensitive to $A\beta_{1-42}$. $A\beta_{1-42}$ at concentrations as low as 10 nM will induce rods in approximately one-half of the sensitive population, which plateaus at a maximum of ~19% for the highest nonlethal concentrations (1 μM).

Hippocampal neurons (6 div) were treated with 1 μM $A\beta_{1-42}$ preparations, fixed at various times, and immunostained for rods. No more than 2% of the neurons in untreated, vehicle-treated, and scrambled peptide-treated control cultures contained rods at any time point. All Aβ samples induced significant rod formation by 6 h after treatment, with maximal rod formation occurring by 12–48 h after treatment (Fig. 2*c*). An increase in rod formation was observed in cultures exposed to 1 μM $A\beta_{1-42}$ large oligomer preparation as early as 2 h after treatment; however, because of the variability in the number of responding cells, this increase did not become significant over untreated controls until 6 h. In these experiments, neuronal survival seldom dropped below 80% at 72 h.

In response to ATP depletion, >80% of hippocampal neurons form rods immediately (Minamide et al., 2000). In contrast, rod formation induced by $A\beta_{1-42}$ exposure occurred in a maximum of only 19% of cultured hippocampal neurons, even with Aβ at concentrations up to 10 μM or varying lengths of exposure (observed up to 3 d). Because neurons in specific subregions of the hippocampus show differential toxicity to $A\beta_{1-42}$ (Bahr et al., 1998; Lambert et al., 1998; Kim et al., 2003), we determined

whether rod formation simply reflected subregion-specific toxicity to $A\beta_{1-42}$. Accordingly, E18 rat hippocampal neurons (6 div) from the CA1 and CA3 regions (supplemental Fig. S1, available at www.jneurosci.org as supplemental material) were treated with 1 μM $A\beta_{1-42}$ large oligomers for 48 h. Controls included dissociated whole hippocampi or enriched CA1 and CA3 neuronal cultures that were either not treated or treated with 1 μM scrambled $A\beta_{1-42}$. No regionally localized population of hippocampal neurons appeared selectively responsive to rod induction by $A\beta_{1-42}$ large oligomers, because a maximum of only 17–18% of the neurons in both CA1- and CA3-enriched cultures contained rods 48 h after treatment (Fig. 2*d*). This maximum percentage response of rod induction for CA1- and CA3-enriched cultures is comparable to the maximum percentage response of rod induction seen for the dissociated, whole hippocampus. Although the percentage of neurons containing rods in control CA1 and CA3 cultures was more than twice the normal control value, we attribute this to the additional stress imposed by the lengthier dissection protocol required to isolate the CA1- and CA3-enriched regions.

Aβ induces ADF/cofilin activation only in neurons that form rods

The level of active (dephosphorylated) ADF/cofilin increases in neurons before and during rod induction by oxidative stress, excitotoxicity, and ischemia (Minamide et al., 2000). To determine whether ADF/cofilin dephosphorylation also accompanies Aβ-induced rod formation, we compared the relative levels of pAC to total cofilin (pAC/total cofilin ratio) in untreated and Aβ-treated neurons. The ratio of the relative fluorescence was compared between the soma and neurites of neurons with and without rods. E18 rat hippocampal neurons (6 div) were treated with 1 μM $A\beta_{1-42}$ large oligomers for 48 h to induce rods before fixing and immunostaining for total cofilin and pAC. In neurons that formed rods, there is a more than twofold reduction in the pAC/total cofilin ratio in the soma of neurons containing rods compared with neurons without rods (Fig. 3), indicating cofilin activation. Furthermore, neurons that do not respond to Aβ treatment by forming rods show no significant change ($p > 0.1$) in the pAC/total cofilin ratio within their soma.

The pAC/total cofilin ratio was also measured within neurites from untreated neurons without rods, from Aβ large oligomer-treated neurons without rods, and from Aβ large oligomer-treated neurons with rods. In untreated neurons without rods, the pAC/total cofilin ratio remained comparable to controls. Similarly, treated neurons without rods also do not exhibit a significant change in the pAC/total cofilin ratio (Fig. 3, no rods). In treated neurons with rods, we examined within the same neuron two groups of neurites: those containing rods and those not containing rods. Within neurites without rods from treated neurons that contained rods elsewhere, a 2.5-fold decline in the pAC/cofilin ratio was observed, similar to what was observed for their soma. However, within neurites containing rods, this ratio declined nearly sevenfold compared with untreated controls (Fig. 3). Furthermore, we observed a >60-fold decline in the pAC/cofilin ratio in the region occupied by the rods (Fig. 3). These data indicate that rod formation and dephosphorylation (activation) of ADF/cofilin in response to Aβ treatment occurs within the same neuronal population.

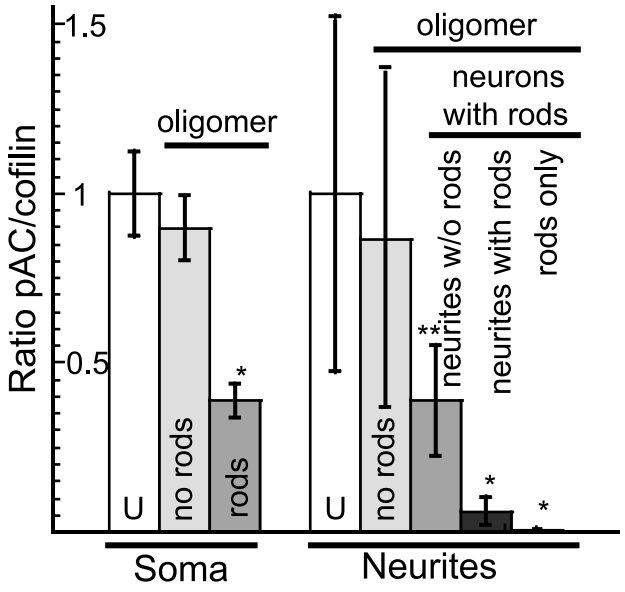

Figure 3. Ratios of phospho-ADF/cofilin to total cofilin staining in neurons in response to treatment with Aβ large oligomers. Rod formation is accompanied by an activation of the available ADF/cofilin pool as indicated by decreasing pAC levels. All values were normalized to the ratio of pAC to total cofilin in untreated neurons (set to 1). Error bars indicate SD. *$p <$ 0.0001 and **$p < 0.05$, significant differences between the control and experimental groups. Neurons with rods in right panel were analyzed in three ways. Ratios were taken from neurites that did not contain rods, from neurites that contained rods but from a non-rod region, and from neurites that contained rods from the region of the rod. U, Untreated neurons; no rods, Aβ-treated neurons that did not form rods.

Localization of endogenous APP, BACE, PS1, and β-secretase cleaved APP to rods

To determine whether rods affect the transport of APP-containing vesicles and the enzymes that process APP into Aβ peptides, we immunostained E18 rat hippocampal neurons with antibodies to the midregion of the APP ectodomain (Koo and Squazzo, 1994; Yamazaki et al., 1996) and to ADF/cofilin. In untreated cells, ADF/cofilin localized predominantly to growth cones and the cell body (Fig. 4*a*,*j*). APP was found in the cell body, but immunostaining was stronger in neurites (Fig. 4*b*), consistent with previous studies (Yamazaki et al., 1995). Rods were induced either by transient (20 min) ATP depletion, followed by washout and overnight recovery (Fig. 4*d–f*), or by adenoviral mediated overexpression of XAC-GFP, which induced spontaneous rod formation by 60 h after infection (Bernstein, Chen, Boyle, and Bamburg, unpublished observations). Minamide et al. (2000) showed that in ATP-depleted neurons, ATP levels returned to normal within 30 min after wash out, but rods reformed during the next 24 h in some neurites from ~30% of the neurons. ADF/cofilin accumulated in rods (Fig. 4*d*,*g–i*), which were also the major site for APP accumulation in a vesicular (punctate) staining pattern (Fig. 4*e*). APP immunostaining either localized along the sides of the rods or was enriched at the distal ends of rods, suggesting accumulation of retrogradely transported vesicles (Fig. 4*f–i*). The β-secretase-cleaved APP (β-C-terminal fragment and/or Aβ), immunostained using an antibody to the N-terminal asp residue of the Aβ peptide, was similarly localized (Fig. 4*j–r*). In untreated cells, β-secretase-cleaved APP was distributed within the cell body and neurites (Fig. 4*k*). In neurites with rods, β-secretase-cleaved APP accumulated either throughout the rods proper or predominantly at one end (Fig. 4*o–r*).

BACE and PS1 immunostaining localized throughout the

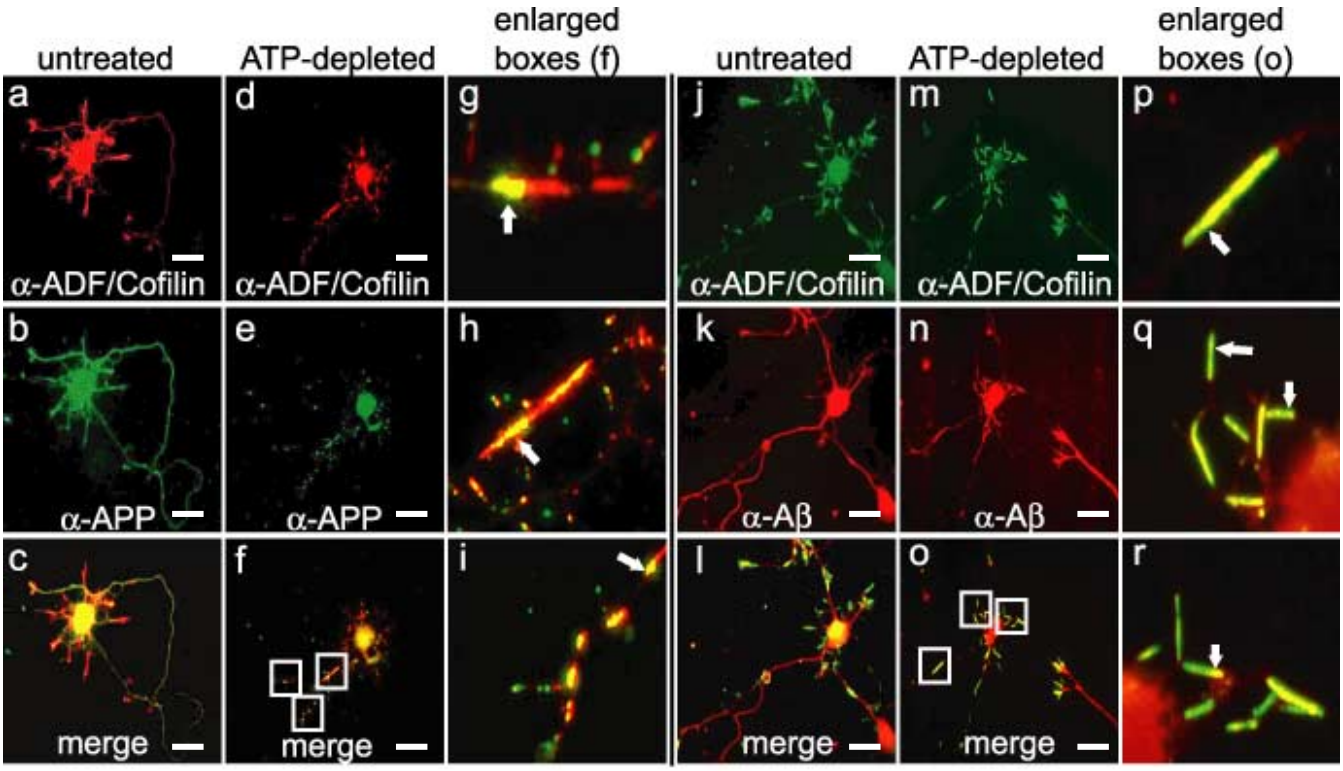

Figure 4. ***a–r***, Vesicles containing APP and the β-secretase-cleaved APP (β-C-terminal fragment or Aβ) accumulate at ADF/cofilin-containing rods in neurites. Untreated E18 rat hippocampal neurons and 20 min ATP-depleted neurons that had undergone a 24 h recovery were fixed 7 div and immunostained as labeled. Scale bars, 10 μm.

soma and neurites in vesicle-like puncta in untreated neurons (supplemental Fig. S5, available at www.jneurosci.org as supplemental material). In neurons with rods, PS1 and BACE localize near rod ends, particularly the distal end and along the side of rods in vesicular-like clusters (supplemental Fig. S5, available at www.jneurosci.org as supplemental material). These data suggest that ADF/cofilin-actin rods are a site for the accumulation of cargo containing APP, BACE, and PS1. We cannot be certain that the biochemical machinery required for Aβ production is completely contained within the same vesicle population. However, from the presence of the β-secretase-cleaved APP in the same location, we can infer that BACE is within the APP-containing vesicles and thus rod-induced disruption of transport might provide an environment in which β-cleavage of APP can occur and accumulate.

We quantified, in three separate experiments, the immunofluorescence staining intensities of APP and β-secretase-cleaved APP associated with the rods and in regions distal to or between the rods, as well as in neurites without rods. Two of these experiments used transient ATP depletion with overnight recovery to induce rods, and the third experiment used rods that spontaneously formed from XAC-GFP overexpression. Results from the three experiments were similar, indicating that the amount of APP and β-cleaved APP accumulation at rods is not dependent on the mechanism of rod formation (i.e., whether rods are induce by ATP depletion or by XAC-GFP overexpression). When compared with the staining intensity of neurites without rods for images captured under identical conditions, there is almost a fivefold increase in the APP and a 2.3-fold increase in β-secretase-cleaved APP associated with the rods and an ~40% reduction in the APP and a 60% reduction in β-secretase-cleaved APP in regions between or distal to the rods (Fig. 5).

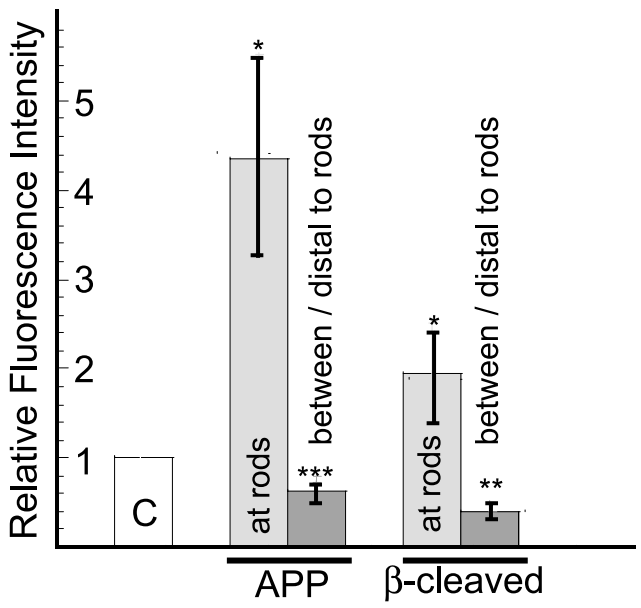

Figure 5. In cultured hippocampal neurons, both APP and β-secretase-cleaved APP accumulate at rods and decline in regions between or distal to rods. Quantitative measurements of average immunofluorescence intensity were obtained for APP and β-secretase-cleaved APP (FCA18 antibody) in cells without rods and in cells in which rods were formed either through transient ATP depletion and 24 h recovery (2 experiments) or from overexpression of XAC-GFP (1 experiment). All images within the same experiment were captured using the same objective, camera, and exposure settings. The fluorescence intensity values for the APP and β-secretase-cleaved APP were set to 1 for the neurites containing no rods (C, control), and relative fluorescence values over the position of the rods (at rods) or between and distal to the rods were measured and plotted relative to the controls. Error bars indicate SEM. *$p < 0.0001$, **$p < 0.002$, or ***$p < 0.09$, significant differences between the control and experimental groups.

Discussion

Actin pathology often accompanies neurodegenerative changes in the brain. Two common actin-containing structures reported in AD brain are Hirano bodies and ADF/cofilin-actin rods. Hirano bodies are large paracrystalline aggregates that contain actin and immunostain for epitopes of ADF/cofilin (Maciver and Harrington, 1995), many actin-binding proteins, and tau (Hirano, 1994). ADF/cofilin-actin rods are much smaller inclusions that often occur in linear arrays. Although it is not known whether the ADF/cofilin-actin rods can recruit additional proteins and give rise to Hirano bodies over time, the two structures are clearly separate entities in fixed AD brain sections (Minamide et al., 2000).

$A\beta_{1-42}$ concentrations as low as 10 nM induce ADF/cofilin-actin rod formation in one-half of the hippocampal neurons that respond to higher concentrations (half-maximum percentage response), the lowest concentration that has been shown to have a physiological effect on neurons (Lambert et al., 1998; Dahlgren et al., 2002; Walsh et al., 2002a; Hiruma et al., 2003; Kim et al., 2003; Takahashi et al., 2004; Cleary et al., 2005). The amount of soluble Aβ extracted from the frontal cortex of control human brains is 0.09 ± 0.05 μg/g and from AD brain is 0.29 ± 0.25 μg/g (McLean et al., 1999). Estimating a 200 μl/g interstitial volume (or 800 μl/g total volume) of water, interstitial concentrations of soluble Aβ are 44–155 nM in control brain and 44–598 nM in AD brain. If Aβ is equally distributed intracellularly and extracellularly, the concentrations are 5–39 nM in control brain and 5–150 nM in AD brain. Reports of decreased soluble Aβ within the CSF of AD patients imply that much of the increased total soluble Aβ-pool in the brain is intracellular (Blennow et al., 2001). In either case, an ~3.5-fold increase in soluble Aβ in AD brain could apply a significant stress on a selective population of sensitive neurons. Rods were not observed in control human brain tissues (Minamide et al., 2000), although the estimated Aβ amounts in these brains is above the minimum concentrations we found necessary to induce rods in cultured hippocampal neurons. This finding suggests that either the form of Aβ in control human brain is different (perhaps a less toxic monomer) (Kim et al., 2003) or alternatively that neurons from control brain are less stressed by other factors (e.g., excess glutamate) that also contribute to rod formation.

Our findings of ADF/cofilin rods in the perfusion-fixed Tg2576 mice are significant because previous studies showing these inclusions in human AD brain could only be performed on brain samples obtained 2–12 h postmortem. Here, the animals were rapidly killed and perfusion fixed, making it much more unlikely that rods formed only as a result of postmortem changes.

Actin dynamics in cultured embryonic neurons use ~50% of cellular ATP (Bernstein and Bamburg, 2003), and thus rods have been proposed to represent an early neuroprotective mechanism during times of transient stress by sequestering virtually all of the ADF/cofilin into nondynamic polymers of ADF/cofilin-ADP-actin (Bernstein, Chen, Boyle, and Bamburg, unpublished observations). The reduction in pAC levels in both soma and neurites of Aβ-treated neurons containing rods is indicative of a global activation of ADF/cofilin proteins within the Aβ-sensitive neuronal population, which may suggest that this subpopulation of neurons has activated a neuroprotective pathway that they were unable to reverse.

The reason for Aβ-induced rod formation in only a subpopulation of cultured hippocampal neurons is still uncharacterized. All cultured hippocampal neurons are responsive to $A\beta_{1-42}$, because treatment with high concentrations of $A\beta_{1-42}$ large oligomers (10 μM) results in complete lethality. Therefore, lower concentrations of $A\beta_{1-42}$ that trigger rod formation must work in a more specific manner on a particularly sensitive group of neurons. There are a number of plausible and potentially interesting mechanisms at work, which may explain this phenomenon. Aβ selectively binds to an undetermined subpopulation of neurons in culture that represents only 30–50% of the total population (Lacor et al., 2004), providing one possible explanation for the limited pool of sensitive neurons. In addition, a subset (30–40%) of cultured hippocampal neurons, susceptible to nerve growth factor-induced apoptosis, expresses the p75 receptor without expression of the cognate Trk receptors (Friedman, 2000). The p75 receptor has been implicated in Aβ-mediated cell death (Perini et al., 2002); thus, Aβ binding to such a subpopulation of neurons may explain the selective response of rod formation.

The aggregation state of Aβ may dictate the substrate binding preference, as suggested by differential binding to NMDA versus non-NMDA receptors (Ye et al., 2004), further narrowing this pool of sensitive neurons. Alternatively, Aβ may affect the activity of upstream regulators of ADF/cofilin. Low levels of $A\beta_{1-42}$ induce rapid Rac1 activation in PC12 cells (Chromy et al., 2003). Hippocampal neurons treated with soluble Aβ also show activation of Rac1/Cdc42 and Pak1 and dephosphorylation of ADF/cofilin proteins enhanced by the phosphatase slingshot, resulting in actin reorganization (Mendoza-Naranjo, Otth, Bamburg, Maccioni, and Gonzalez-Billault, unpublished observations). Therefore, Aβ peptides may induce activation of specific signaling pathways in a subpopulation of normal neurons that results in enhanced ADF/cofilin activity. In addition, Aβ has been shown to have detrimental effects on mitochondria (Grant et al., 1999; Anandatheerthavarada et al., 2003; Lustbader et al., 2004; Mattson, 2004), and there may exist a neuronal subpopulation in which mitochondria are extremely sensitive to Aβ. The ability to visualize rod-containing neurons in live cells expressing fluorescent protein chimeras of ADF/cofilin offers an opportunity to isolate and characterize this selective neuronal population.

In cultured neurons, $A\beta_{1-42}$ peptides induce rods that become sites for the accumulation of vesicles containing APP and its proteolytic processing machinery. In brains of transgenic mice expressing the Swedish mutation of human APP, one of the earliest defects observed is an accumulation of vesicular and organelle cargoes and formation of axonal varicosities at sites of transport blockage (Stokin et al., 2005). Maximal production of Aβ from APP in cultured neurons requires the endocytosis of APP (Koo and Squazzo, 1994; Cordy et al., 2003; Ehehalt et al., 2003). Inhibition of endocytosis in hippocampal neurons by expression of dominant interfering forms of dynamin, a GTPase required for endocytosis, dramatically decreases the amount of Aβ peptides that are secreted into the cell-culture medium (Ehehalt et al., 2003). The accumulation of APP, BACE, and PS1 in vesicles accumulating at rods may be a mechanism by which rods could enhance production of Aβ peptides. It is particularly noteworthy that the APP-containing vesicles either reside evenly distributed along the rods or accumulate at the distal end of the rod, suggesting that retrogradely transported endosomes accumulate. Aβ oligomers occur in vesicles localized along neurites and at synaptic compartments in both cultured neurons and in the brains of Tg2576 mice (Takahashi et al., 2004). Rods provide an attractive mechanism to describe a variety of pathological and experimental data implicating the blockage of cargo transport in neurodegenerative diseases.

From the combined data presented here and from the findings

of others, we propose a hypothetical feedforward model (supplemental Fig. S6, available at www.jneurosci.org as supplemental material) for neurodegeneration and senile plaque growth in AD and potentially in other amyloidogenic disorders, such as Down syndrome (Head and Lott, 2004; Nixon, 2005). A specific neuronal subpopulation may be adversely susceptible to the accumulation of Aβ, such as in FAD, or to other stress inducers such as ischemia, oxidative stress, or excitotoxicity, which may be involved in sporadic AD. These insults can result in rod formation within neurites, thereby blocking vesicle transport and leading to the continued generation of Aβ within stalled endosomes, and subsequent secretion at these focal sites. Locally elevated Aβ can give rise to additional rod formation in the surrounding neuropil, further exacerbating the neurodegenerative cycle.

References

Abe H, Ohshima S, Obinata T (1989) A cofilin-like protein is involved in the regulation of actin assembly in developing skeletal muscle. J Biochem (Tokyo) 106:696–702.

Anandatheerthavarada HK, Biswas G, Robin MA, Avadhani NG (2003) Mitochondrial targeting and a novel transmembrane arrest of Alzheimer's amyloid precursor protein impairs mitochondrial function in neuronal cells. J Cell Biol 161:41–54.

Bahr BA, Hoffman KB, Yang AJ, Hess US, Glabe CG, Lynch G (1998) Amyloid beta protein is internalized selectively by hippocampal field CA1 and causes neurons to accumulate amyloidogenic carboxyterminal fragments of the amyloid precursor protein. J Comp Neurol 397:139–147.

Bamburg JR, Wiggan OP (2002) ADF/cofilin and actin dynamics in disease. Trends Cell Biol 12:598–605.

Bartlett WP, Banker GA (1984) An electron microscopic study of the development of axons and dendrites by hippocampal neurons in culture. I. Cells which develop without intercellular contacts. J Neurosci 4:1944–1953.

Bernstein BW, Bamburg JR (2003) Actin-ATP hydrolysis is a major energy drain for neurons. J Neurosci 23:1–6.

Blennow K, Vanmechelen E, Hampel H (2001) CSF total tau, Abeta42 and phosphorylated tau protein as biomarkers for Alzheimer's disease. Mol Neurobiol 24:87–97.

Bruijn LI, Becher MW, Lee MK, Anderson KL, Jenkins NA, Copeland NG, Sisodia SS, Rothstein JD, Borchelt DR, Price DL, Cleveland DW (1997) ALS-linked SOD1 mutant G85R mediates damage to astrocytes and promotes rapidly progressive disease with SOD1-containing inclusions. Neuron 18:327–338.

Cafe C, Torri C, Bertorelli L, Angeretti N, Lucca E, Forloni G, Marzatico F (1996) Oxidative stress after acute and chronic application of beta-amyloid fragment 25–35 in cortical cultures. Neurosci Lett 203:61–65.

Chartier-Harlin MC, Crawford F, Hamandi K, Mullan M, Goate A, Hardy J, Backhovens H, Martin JJ, Broeckhoven CV (1991a) Screening for the beta-amyloid precursor protein mutation (APP717: Val–Ile) in extended pedigrees with early onset Alzheimer's disease. Neurosci Lett 129:134–135.

Chartier-Harlin MC, Crawford F, Houlden H, Warren A, Hughes D, Fidani L, Goate A, Rossor M, Roques P, Hardy J, Mullan M (1991b) Early-onset Alzheimer's disease caused by mutations at codon 717 of the beta-amyloid precursor protein gene. Nature 353:844–846.

Chromy BA, Nowak RJ, Lambert MP, Viola KL, Chang L, Velasco PT, Jones BW, Fernandez SJ, Lacor PN, Horowitz P, Finch CE, Krafft GA, Klein WL (2003) Self-assembly of Abeta (1–42) into globular neurotoxins. Biochemistry 42:12749–12760.

Cleary JP, Walsh DM, Hofmeister JJ, Shankar GM, Kuskowski MA, Selkoe DJ, Ashe KH (2005) Natural oligomers of the amyloid-beta protein specifically disrupt cognitive function. Nat Neurosci 8:79–84.

Cordy JM, Hussain I, Dingwall C, Hooper NM, Turner AJ (2003) Exclusively targeting beta-secretase to lipid rafts by GPI-anchor addition up-regulates beta-site processing of the amyloid precursor protein. Proc Natl Acad Sci USA 100:11735–11740.

Dahlgren KN, Manelli AM, Stine Jr WB, Baker LK, Krafft GA, LaDu MJ (2002) Oligomeric and fibrillar species of amyloid-beta peptides differentially affect neuronal viability. J Biol Chem 277:32046–32053.

Ehehalt R, Keller P, Haass C, Thiele C, Simons K (2003) Amyloidogenic processing of the Alzheimer beta-amyloid precursor protein depends on lipid rafts. J Cell Biol 160:113–123.

Friedman WJ (2000) Neurotrophins induce death of hippocampal neurons via the p75 receptor. J Neurosci 20:6340–6346.

Goate A, Chartier-Harlin MC, Mullan M, Brown J, Crawford F, Fidani L, Giuffra L, Haynes A, Irving N, James L, Mant R, Newton P, Rooke K, Roques P, Talbot C, Pericak-Vance M, Roses A, Williamson R, Rossor M, Owen M, Hardy J (1991) Segregation of a missense mutation in the amyloid precursor protein gene with familial Alzheimer's disease. Nature 349:704–706.

Gong Y, Chang L, Viola KL, Lacor PN, Lambert MP, Finch CE, Krafft GA, Klein WL (2003) Alzheimer's disease-affected brain: presence of oligomeric A beta ligands (ADDLs) suggests a molecular basis for reversible memory loss. Proc Natl Acad Sci USA 100:10417–10422.

Grace EA, Rabiner CA, Busciglio J (2002) Characterization of neuronal dystrophy induced by fibrillar amyloid beta: implications for Alzheimer's disease. Neuroscience 114:265–273.

Grant SM, Shankar SL, Chalmers-Redman RM, Tatton WG, Szyf M, Cuello AC (1999) Mitochondrial abnormalities in neuroectodermal cells stably expressing human amyloid precursor protein (hAPP751). NeuroReport 10:41–46.

Hardy J, Selkoe DJ (2002) The amyloid hypothesis of Alzheimer's disease: progress and problems on the road to therapeutics. Science 297:353–356.

Harris ME, Hensley K, Butterfield DA, Leedle RA, Carney JM (1995) Direct evidence of oxidative injury produced by the Alzheimer's beta-amyloid peptide (1–40) in cultured hippocampal neurons. Exp Neurol 131:193–202.

Hartley DM, Walsh DM, Ye CP, Diehl T, Vasquez S, Vassilev PM, Teplow DB, Selkoe DJ (1999) Protofibrillar intermediates of amyloid β-protein induce acute electrophysiological changes and progressive neurotoxicity in cortical neurons. J Neurosci 19:8876–8884.

Head E, Lott IT (2004) Down syndrome and beta-amyloid deposition. Curr Opin Neurol 17:95–100.

Hensley K, Butterfield DA, Hall N, Cole P, Subramaniam R, Mark R, Mattson MP, Markesbery WR, Harris ME, Aksenov M, Askenova M, Wu JF, Carney JM (1996) Reactive oxygen species as causal agents in the neurotoxicity of the Alzheimer's disease-associated amyloid beta peptide. Ann NY Acad Sci 786:120–134.

Hirano A (1994) Hirano bodies and related neuronal inclusions. Neuropathol Appl Neurobiol 20:3–11.

Hiruma H, Katakura T, Takahashi S, Ichikawa T, Kawakami T (2003) Glutamate and amyloid β-protein rapidly inhibit fast axonal transport in cultured rat hippocampal neurons by different mechanisms. J Neurosci 23:8967–8977.

Hsiao K, Chapman P, Nilsen S, Eckman C, Harigaya Y, Younkin S, Yang F, Cole G (1996) Correlative memory deficits, Abeta elevation, and amyloid plaques in transgenic mice. Science 274:99–102.

Kim HJ, Chae SC, Lee DK, Chromy B, Lee SC, Park YC, Klein WL, Krafft GA, Hong ST (2003) Selective neuronal degeneration induced by soluble oligomeric amyloid beta protein. FASEB J 17:118–120.

Koo EH, Squazzo SL (1994) Evidence that production and release of amyloid beta-protein involves the endocytic pathway. J Biol Chem 269:17386–17389.

Lacor PN, Buniel MC, Chang L, Fernandez SJ, Gong Y, Viola KL, Lambert MP, Velasco PT, Bigio EH, Finch CE, Krafft GA, Klein WL (2004) Synaptic targeting by Alzheimer's-related amyloid β oligomers. Neurobiol Dis 24:10091–10200.

Lambert MP, Barlow AK, Chromy BA, Edwards C, Freed R, Liosatos M, Morgan TE, Rozovsky I, Trommer B, Viola KL, Wals P, Zhang C, Finch CE, Krafft GA, Klein WL (1998) Diffusible, nonfibrillar ligands derived from Abeta1–42 are potent central nervous system neurotoxins. Proc Natl Acad Sci USA 95:6448–6453.

Lim GP, Calon F, Morihara T, Yang F, Teter B, Ubeda O, Salem Jr N, Frautschy SA, Cole GM (2005) A diet enriched with the omega-3 fatty acid docosahexaenoic acid reduces amyloid burden in an aged Alzheimer mouse model. J Neurosci 25:3032–3040.

Lustbader JW, Cirilli M, Lin C, Xu HW, Takuma K, Wang N, Caspersen C, Chen X, Pollak S, Chaney M, Trinchese F, Liu S, Gunn-Moore F, Lue LF, Walker DG, Kuppusamy P, Zewier ZL, Arancio O, Stern D, Yan SS, et al. (2004) ABAD directly links Abeta to mitochondrial toxicity in Alzheimer's disease. Science 304:448–452.

Maciver SK, Harrington CR (1995) Two actin binding proteins, actin depo-

lymerizing factor and cofilin, are associated with Hirano bodies. NeuroReport 6:1985–1988.
Mattson MP (2004) Pathways towards and away from Alzheimer's disease. Nature 430:631–639.
Mattson MP, Kater SB (1988) Isolated hippocampal neurons in cryopreserved long-term cultures: development of neuroarchitecture and sensitivity to NMDA. Int J Dev Neurosci 6:439–452.
McLean CA, Cherny RA, Fraser FW, Fuller SJ, Smith MJ, Beyreuther K, Bush AI, Masters CL (1999) Soluble pool of Abeta amyloid as a determinant of severity of neurodegeneration in Alzheimer's disease. Ann Neurol 46:860–866.
Meberg PJ, Bamburg JR (2000) Increase in neurite outgrowth mediated by overexpression of actin depolymerizing factor. J Neurosci 20:2459–2469.
Meberg PJ, Miller MW (2003) Culturing hippocampal and cortical neurons. Methods Cell Biol 71:111–127.
Meberg PJ, Ono S, Minamide LS, Takahashi M, Bamburg JR (1998) Actin depolymerizing factor and cofilin phosphorylation dynamics: response to signals that regulate neurite extension. Cell Motil Cytoskeleton 39:172–190.
Minamide LS, Striegl AM, Boyle JA, Meberg PJ, Bamburg JR (2000) Neurodegenerative stimuli induce persistent ADF/cofilin-actin rods that disrupt distal neurite function. Nat Cell Biol 2:628–636.
Murrell J, Farlow M, Ghetti B, Benson MD (1991) A mutation in the amyloid precursor protein associated with hereditary Alzheimer's disease. Science 254:97–99.
Nixon RA (2005) Endosome function and dysfunction in Alzheimer's disease and other neurodegenerative diseases. Neurobiol Aging 26:373–382.
Perini G, Della-Bianca V, Politi V, Della valle G, Dal-Pra I, Rossi F, Armato U (2002) Role of p75 neurotrophin receptor in the neurotoxicity by beta-amyloid peptides and synergistic effect of inflammatory cytokines. J Exp Med 195:907–918.
Pike CJ, Cummings BJ, Cotman CW (1992) Beta-amyloid induces neuritic dystrophy in vitro: similarities with Alzheimer pathology. NeuroReport 3:769–772.
Price DL, Sisodia SS, Gandy SE (1995) Amyloid beta amyloidosis in Alzheimer's disease. Curr Opin Neurol 8:268–274.
Sisodia SS, Price DL (1995) Role of the beta-amyloid protein in Alzheimer's disease. FASEB J 9:366–370.
Stine Jr WB, Dahlgren KN, Krafft GA, LaDu MJ (2003) In vitro characterization of conditions for amyloid-beta peptide oligomerization and fibrillogenesis. J Biol Chem 278:11612–11622.
Stokin GB, Lillo C, Falzone TL, Brusch RG, Rockenstein E, Mount SL, Raman R, Davies P, Masliah E, Williams DS, Goldstein LS (2005) Axonopathy and transport deficits early in the pathogenesis of Alzheimer's disease. Science 307:1282–1288.
Takahashi RH, Almeida CG, Kearney PF, Yu F, Lin MT, Milner TA, Gouras GK (2004) Oligomerization of Alzheimer's β-amyloid within processes and synapses of cultured neurons and brain. J Neurosci 24:3592–3599.
Tanzi RE, Bertram L (2005) Twenty years of the Alzheimer's disease amyloid hypothesis: a genetic perspective. Cell 120:545–555.
Walsh DM, Hartley DM, Kusumoto Y, Fezoui Y, Condron MM, Lomakin A, Benedek GB, Selkoe DJ, Teplow DB (1999) Amyloid beta-protein fibrillogenesis. Structure and biological activity of protofibrillar intermediates. J Biol Chem 274:25945–25952.
Walsh DM, Klyubin I, Fadeeva JV, Cullen WK, Anwyl R, Wolfe MS, Rowan MJ, Selkoe DJ (2002a) Naturally secreted oligomers of amyloid beta protein potently inhibit hippocampal long-term potentiation in vivo. Nature 416:535–539.
Walsh DM, Klyubin I, Fadeeva JV, Rowan MJ, Selkoe DJ (2002b) Amyloid-beta oligomers: their production, toxicity and therapeutic inhibition. Biochem Soc Trans 30:552–557.
Yamazaki T, Selkoe DJ, Koo EH (1995) Trafficking of cell surface beta-amyloid precursor protein: retrograde and transcytotic transport in cultured neurons. J Cell Biol 129:431–442.
Yamazaki T, Koo EH, Selkoe DJ (1996) Trafficking of cell-surface amyloid beta-protein precursor. II. Endocytosis, recycling and lysosomal targeting detected by immunolocalization. J Cell Sci 109:999–1008.
Ye C, Walsh DM, Selkoe DJ, Hartley DM (2004) Amyloid β-protein induced electrophysiological changes are dependent on aggregation state: *N*-methyl-D-aspartate (NMDA) versus non-NMDA receptor/channel activation. Neurosci Lett 366:320–325.